Luminescence Properties of Salts of the $[Pt(trpy)Cl]^+$ and $[Pt(trpy)(MeCN)]^{2+}$ Chromophores: Crystal Structure of $[Pt(trpy)(MeCN)](SbF_6)_2$

Riaan Büchner, John S. Field,* and Raymond J. Haines

Department of Chemistry, University of Natal, Private Bag X01, Pietermaritzburg, South Africa 3209

Corey T. Cunningham and David R. McMillin*,†

Department of Chemistry, 1393 Brown Building, Purdue University, West Lafayette, Indiana 47907-1393

Received August 30, 1996[⊗]

The crystal structure of $[Pt(trpy)(MeCN)](SbF_6)_2$, where trpy denotes 2,2′:6′,2″-terpyridine, shows that the platinum complex packs as a monomer; however, the $^3\pi-\pi^*$ emission of the solid occurs at surprisingly long wavelengths at room temperature. At lower temperatures new, shorter-wavelength maxima appear. Of the known salts with the composition [Pt(trpy)Cl]A, the $A = SbF_6^-$ system is the lone example that exhibits a temperature-independent emission maximum. In these platinum(II) terpyridines, energy migration to defects or trap sites is one of the phenomena responsible for the temperature dependence of the solid-state emission spectrum. If trap emission is evident, the low-temperature spectral data are most representative of the bulk material.

Introduction

Luminescent, square-planar complexes of Pt(II) containing α,α′-diimine ligands have intriguing spectroscopic and photophysical properties.[1] In a monomeric environment, such as in a dilute glass solution, the complexes may exhibit emission from intraligand[2] (IL), metal-to-ligand-charge-transfer[3] (MLCT), or ligand-field[3] (LF) states. Because these states are of similar energy, the relative ordering is sensitive to factors such as ligand field strength, diimine substituents, and the nature of the coligands. In the solid state, Pt−Pt or $\pi-\pi$ interactions between chromophores often have a strong influence on the emission. Three idealized solid-state structure types occur: *monomeric* structures in which the Pt−Pt distances are all greater than 4.5 Å; *linear-chain structures* in which the Pt(II) complexes are stacked equidistantly (Pt−Pt separations of 3.2−3.4 Å) along an axis that is usually, but not always, perpendicular to the plane of the complex; and *dimer* structures in which the Pt complexes segregate into pairs.[1] Compounds with monomeric structures display luminescence properties similar to those observed in dilute solutions. On the other hand, those with linear-chain structures typically exhibit $\pi^*(L) \rightarrow d\sigma^*$ emissions from metal−metal-to-ligand-charge-transfer (MMLCT) excited states.[1] With these systems, the emission undergoes a characteristic red shift at lower temperatures due to a decrease in the mean Pt−Pt spacing.[4] Compounds with dimer structures also typically exhibit MMLCT emissions, but less information is available about the temperature-dependent properties. However, one study reported that the emissions from a series of ligand-bridged dimers blue-shift when the temperature drops from ambient to 77 K.[5]

By and large, Pt(II) complexes of the tridentate 2,2′:6′,2″-terpyridine (trpy) ligand possess luminescence properties much like those of the corresponding α,α′-diimine complexes. For example, Yip et al. have reported the properties of the $[Pt(trpy)Cl]CF_3SO_3$ salt at room temperature as well as 77 K, and they found that the emission maximum red-shifted at the lower temperature.[6] More recently, Bailey et al. examined the photophysical properties of a series of salts containing the $[Pt(trpy)Cl]^+$ moiety.[7] They assigned the low-temperature solid-state luminescence of these salts to ^{3}MMLCT states, and they concluded that the emission energy varied with the counterion (ClO_4^-, Cl^-, $CF_3SO_3^-$, or PF_6^-) because of differences in the Pt−Pt and $\pi-\pi$ interactions in the lattice.[7] Contrary to the results of Yip et al., however, for all except the red perchlorate salt, Bailey et al. reported that the emission narrowed and exhibited a blue shift with a decrease in temperature.

The present report deals with the temperature dependence of the emissions from $[Pt(trpy)Cl]SbF_6$ and $[Pt(trpy)Cl]CF_3SO_3$ in the solid state as well as the crystal structure and emission spectrum of $[Pt(trpy)(MeCN)](SbF_6)_2$. The acetonitrile adduct exhibits a triplet emission (^{3}IL parentage) from the solid, but the energy varies with temperature due to the participation of various trap centers.

Experimental Section

Materials and Syntheses. The purity of all reagent grade materials was adequate as received. The $Pt(PhCN)_2Cl_2$ starting complex and 2,2′:6′,2″-terpyridine (trpy) were obtained from Strem Chemicals, while the salts $AgSbF_6$ and $AgCF_3SO_3$ were from Fluka AG. Successive fractional distillations over sodium octanolate and sulfuric acid served

† E-mail: mcmillin@purdue.edu. Fax: (765) 494-0239.

⊗ Abstract published in *Advance ACS Abstracts,* August 15, 1997.

(1) Houlding, V. H.; Miskowski, V. M. *Coord. Chem. Rev.* **1991**, *111*, 145−152.
(2) Miskowski, V. M.; Houlding, V. H. *Inorg. Chem.* **1989**, *28*, 1529−1533. Miskowski, V. M.; Houlding, V. H. *Inorg. Chem.* **1991**, *30*, 4446−4452.
(3) Miskowski, V. M.; Houlding, V. H; Che, C. M.; Wang, Y. *Inorg Chem.* **1993**, *32*, 2518−2524.
(4) Biedermann, J.; Wallfahrer, M.; Gliemann, G. *J. Lumin.* **1987**, *37*, 323−329. Schwarz, R.; Lindner, M.; Gliemann, G. *Ber. Bunsen-Ges Phys. Chem.* **1987**, *91*, 1233−1237.
(5) Bailey, J. A.; Miskowski, V. M.; Gray, H. B. *Inorg. Chem.* **1993**, *32*, 369−370.
(6) Yip, H. K.; Cheng, L. K.; Cheung, K. K.; Che, C. M. *J. Chem. Soc., Dalton Trans.* **1993**, 2933−2938.
(7) Bailey, J. A.; Hill, M. G.; Marsh, R. E.; Miskowski, V. M.; Schaefer, W. P.; Gray, H. B. *Inorg. Chem.* **1995**, *34*, 4591−4599.

S0020-1669(96)01068-3 CCC: $14.00

to purify acetonitrile, but analytical grade solvents sufficed in all other cases.

[Pt(trpy)Cl]A (A = SbF_6^-, or $CF_3SO_3^-$). The preparation began with the addition of an equimolar amount of AgA (0.146 g for A = SbF_6^-, 0.109 g for A = $CF_3SO_3^-$; 0.424 mmol) in MeCN (5−7 cm^3) to a suspension of $Pt(PhCN)_2Cl_2$ (0.200 g, 0.424 mmol) in MeCN (15 cm^3). After a 15 h reflux and a filtration step, came the addition of a 5% excess of 2,2′:6′,2″-terpyridine (0.104 g, 0.445 mmol) and another 15 h reflux. A second filtration removed any additional AgCl precipitate prior to the removal of solvent. Finally, treatment with hot MeCN provided for the extraction of the [Pt(trpy)Cl]A salt. Slow cooling of the MeCN solution resulted in the precipitation of a crystalline solid of bright orange (A = SbF_6^-) or orange (A = $CF_3SO_3^-$) material. Washing the bright orange SbF_6^- salt with acetone effected a color change to bright yellow but did not alter the color of the other salt. Yield: 70−80%. Anal. Calcd (for A = SbF_6^-): C, 25.75; H, 1.58; N, 6.00. Found: C, 25.88, H, 1.67; N, 6.05. Calcd (for A = $CF_3SO_3^-$): C, 31.36; H, 1.81; N, 6.86. Found: C, 30.97; H, 1.67; N, 7.27. IR (KBr; cm^{-1}): ν(trpy) 1606s, 1480m, 1456s, 1442m, 1400m, 1317m, 1035m, 773s; $\nu(SbF_6^-)$: 656s; [$\nu(CF_3SO_3^-)$]: 1266s, 1158s, 1030s.

[Pt(trpy)(MeCN)$(SbF_6)_2$. A vapor-extraction apparatus facilitated the continuous extraction of solid [Pt(trpy)Cl]SbF_6 (0.300 g, 0.318 mmol) into refluxing acetonitrile containing an excess of $AgSbF_6$ (0.291 g, 0.848 mmol). When all the [Pt(trpy)Cl]SbF_6 had dissolved (after *ca.* 4 h) and the solution had cooled to room temperature, filtration removed the precipitated AgCl. The precipitation of unreacted [Pt(trpy)Cl]SbF_6 occurred as the volume decreased. After filtration, further evaporation led to the deposition of the desired product. The final purification steps involved a wash with acetone and diethyl ether and then exposure to a vacuum. After dissolution in acetonitrile, the crystallization of [Pt(trpy)(MeCN)]$(SbF_6)_2$ as light-yellow block-shaped crystals occurred as the solvent evaporated. Yield: 45%. Anal. Calcd: C, 21.70; H, 1.50; N, 5.95. Found: C, 21.61; H, 1.39; N, 5.93. IR (KBr; cm^{-1}): ν(C≡N) 2332m, 2304w; ν(trpy) 1611s, 1574m, 1510m, 1510w, 1458m, 1455s, 1408m, 1322m, 1250m, 1036m, 783s; $\nu(SbF_6^-)$ 656s.

Methods. For luminescence measurements of solutions, a series of freeze−pump−thaw cycles served to remove dissolved dioxygen. During the steady-state emission studies and the lifetime experiments, a 440 nm long-wave-pass filter protected the detector from scattered light. For the lifetime studies, there was a 337 nm notch filter between the sample and the laser. In the course of the variable-temperature studies, all samples equilibrated at least 1 h after the sensor reached the desired temperature. A standard method of analysis yielded the lifetimes from the emission-decay data as before.[8]

Instrumentation. A Shimadzu FTIR-4300 spectrophotometer provided infrared spectra of samples in KBr disks, and a Perkin-Elmer Lambda 4C and a Hewlett Packard 8452A diode-array spectrophotometer provided the absorbance data. An SLM Aminco SPF-500 instrument yielded the emission results, and a previously described apparatus[9] provided the lifetime data, except that the excitation source was a Laser Science, Inc., Model 337ND-S nitrogen laser. For the variable-temperature emission measurements, the cryostat was an Oxford Instruments Model DN1704 liquid-nitrogen-cooled system complete with an Oxford Instruments temperature controller. For the 77 K data, the sample holder was a quartz finger dewar filled with liquid nitrogen. The diffractometer was an Entraf−Nonius CAD4.

Crystal Structure Determination. The crystal of [Pt(trpy)(MeCN)]$(SbF_6)_2$ used for the diffraction study was a nearly cube-shaped block with dimensions 0.12 × 0.15 × 0.12 mm. The $\omega-\theta$ scan method in conjunction with monochromated Mo Kα radiation yielded cell dimensions and diffraction intensities. A total of 25 reflections with $6 < \theta < 12°$ sufficed for determining cell dimensions. The data out to $2\theta = 46°$ (a total of 3708 reflections) showed monoclinic symmetry and exhibited systematic absences characteristic of the space group $P2_1/c$ (14). Of the 2708 unique reflections, there were 1988 with $I > 3\sigma(I)$ that were useful for the solution and refinement of the structure. The solution of the Patterson function gave the location of the Pt and Sb atoms, and the remaining non-H atoms appeared in a difference Fourier map phased on the heavy atoms. The H atoms appeared in calculated positions. For the purposes of refinement, all atoms, except the H atoms, were assigned anisotropic temperature parameters. The refinement utilized the full-matrix least-squares method and the weighting scheme $w = 1/[\sigma^2(F) + 0.00580F^2]$. Table 1 gives a summary of the crystal parameters and other details of the refinement.

Table 1. Crystal Parameters at 295 K for [Pt(trpy)(MeCN)]$(SbF_6)_2$

empirical formula	$C_{17}H_{14}F_{12}N_4PtSb_2$
fw	940.89
space group (No.)	$P2_1/c$ (14)
temp, °C	22
a, Å	13.705(6)
b, Å	12.324(4)
c, Å	14.507(4)
β, deg	98.27(3)
Z	4
V, $Å^3$	2425.0(16)
ρ_{calcd}, g cm^{-3}	2.58
λ, Å	0.710 73
μ, cm^{-1}	84.18
transm coeff	0.678−0.998
R ($I > 3\sigma(I)$)[a]	0.043 for 1988 reflcns
R_w[a]	0.050 for 1988 reflcns

[a] $R = \sum(|F_o| - |F_c|)/\sum F_o$; $R_w = \sum w^{1/2}(|F_o| - |F_c|)/\sum w^{1/2}F_o$.

Results

The approach used for the synthesis of the chloro-containing derivatives [Pt(trpy)Cl]A (A = SbF_6^-, $CF_3SO_3^-$) was different from that employed by Yip et al.[6] or Bailey et al.[7] in that the neutral compound $Pt(PhCN)_2Cl_2$, rather than the ionic species [Pt(trpy)Cl]Cl, served as the starting material. Thus, treatment of the benzonitrile complex with 1 equiv of the appropriate silver salt in refluxing acetonitrile, followed by addition of a slight excess of terpyridine, afforded an analytically pure product after workup and crystallization from acetonitrile. Interestingly, the SbF_6^- salt separated from acetonitrile as bright orange crystals that converted to yellow crystals over a period of ca. 10 min after the removal of the mother liquor. An instantaneous conversion from the metastable orange modification to the yellow form occurred with an acetone wash. For the synthesis of the acetonitrile salt [Pt(trpy)(MeCN)]$(SbF_6)_2$, [Pt(trpy)Cl]SbF_6 was the starting material. Treatment of a boiling solution of the latter with 2 equiv of $AgSbF_6$ led to the formation of the desired product, along with AgCl and unreacted [Pt(trpy)Cl](SbF_6); the latter selectively precipitated from a cooled acetonitrile solution, allowing the isolation of [Pt(trpy)(MeCN)]$(SbF_6)_2$ as light yellow block-shaped crystals. The solid-state infrared spectrum, measured in a KBr disk, exhibited two peaks in the C−N stretching region at 2330 and 2302 cm^{-1}, each attributable to the MeCN ligand. A similar C−N stretching peak pattern has been observed for $Pt(MeCN)_2Cl_2$.[10] Attempts to synthesize the BF_4^- and $CF_3SO_3^-$ salts of $[Pt(trpy)(MeCN)]^{2+}$ from [Pt(trpy)Cl]A (A = $CF_3SO_3^-$, BF_4^-) were unsuccessful, largely because of the difficulties incurred in the separation of the starting material from the desired product.

Crystal Structure of [Pt(trpy)(MeCN)]$(SbF_6)_2$. The structure shows that the platinum adopts a planar coordination geometry; see Figure 1 for a perspective view of the cation. The positional and thermal parameters as well as the calculated interatomic distances and angles for [Pt(trpy)(MeCN)]$(SbF_6)_2$ appear in Tables 2 and 3. The maximum deviation from the

(8) Liu, F.; Cunningham, K. L.; Uphues, W.; Fink, G. W.; Schmolt, J.; McMilllin, D. R. *Inorg. Chem.* **1995**, *34*, 2015−2018.
(9) Cunningham, K. L.; Hecker, C. R.; McMillin, D. R. *Inorg. Chim. Acta* **1996**, *242*, 143−147.
(10) Rochon, F. D.; Melanson, R.; Howard-Lock, H. E.; Lock, C. J. L.; Turner, G. *Can. J. Chem.* **1984**, *62*, 860−869.

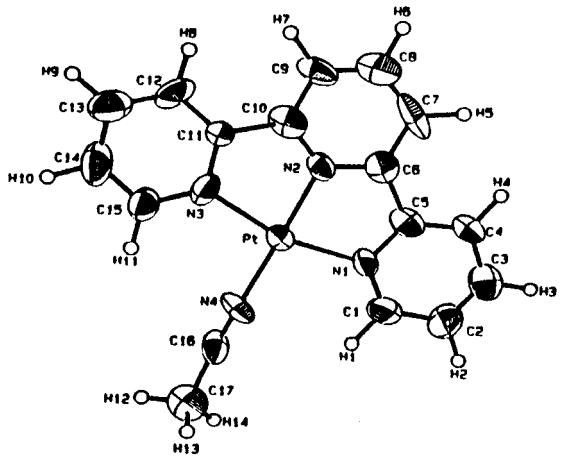

Figure 1. The molecular geometry and atom-numbering scheme employed for the $[Pt(trpy)(MeCN)]^{2+}$ cation. Atom designators are 50% probability ellipsoids except for those of the H atoms, which appear as spheres of arbitrary radius.

Table 2. Positional ($\times 10^4$) and Thermal Parameters ($Å^2 \times 10^3$) for $[Pt(trpy)(MeCN)](SbF_6)_2$

atom	*x*	*y*	*z*	U_{eq}[a]
Pt	2394	2116(1)	4000	42
N1	2983(9)	1172(12)	3058(10)	50(3)
N2	2853(9)	3269(11)	3262(9)	43(3)
N3	1939(10)	3403(10)	4678(11)	53(4)
N4	1906(10)	929(13)	4751(10)	54(4)
C1	3043(14)	106(16)	3024(14)	65(5)
C2	3467(17)	−430(17)	2330(16)	85(7)
C3	3857(13)	147(19)	1709(15)	69(6)
C4	3842(14)	1321(17)	1736(14)	66(5)
C5	3384(12)	1771(15)	2439(13)	52(4)
C6	3322(12)	2963(16)	2546(12)	53(4)
C7	3693(13)	3793(25)	2044(14)	84(7)
C8	3539(17)	4852(21)	2295(18)	81(7)
C9	3062(15)	5091(16)	3004(12)	65(5)
C10	2710(12)	4274(16)	3507(11)	55(5)
C11	2163(11)	4367(13)	4305(12)	44(4)
C12	1889(14)	5311(16)	4648(17)	73(6)
C13	1376(15)	5363(18)	5390(17)	76(6)
C14	1154(14)	4372(21)	5754(17)	86(7)
C15	1446(12)	3413(16)	5419(13)	56(5)
C16	1654(12)	281(13)	5164(13)	57(5)
C17	1314(14)	−673(15)	5700(13)	71(5)
Sb1	4240(1)	−2792(1)	166(1)	58
F1	3589(1)	−4063(1)	150(1)	133(5)
F2	5288(1)	−3468(1)	−188(1)	216(10)
F3	3744(1)	−2567(1)	−1032(1)	198(9)
F4	4897(1)	−1521(1)	195(1)	234(10)
F5	3197(1)	−2110(1)	526(1)	188(9)
F6	4740(1)	−3013(1)	1371(1)	159(7)
Sb2	350(1)	6991(1)	7767(1)	65
F7	−13(1)	6484(1)	6607(1)	221(11)
F8	1549(1)	7322(1)	7490(1)	148(6)
F9	−95(1)	8317(1)	7400(1)	232(11)
F10	701(1)	7489(1)	8937(1)	144(6)
F11	−856(1)	6657(1)	8052(1)	149(6)
F12	785(1)	5661(1)	8144(1)	186(8)

mean plane through the Pt and four bonded N atoms is 0.012 Å for the metal atom. As a consequence of the geometric constraints imposed by the trpy ligand, the angles subtended at the Pt atom deviate from the idealized values of 90 and 180°; the relevant angles are 81.8(6) (N1−Pt−N2), 162.5(6) (N1−Pt−N3), 98.3(6) (N1−Pt−N4), 80.8(6) (N2−Pt−N3), 179.3-(5) (N2−Pt−N4), and 99.1(6)° (N3−Pt−N4). The Pt−N distances are also typical of metal−terpyridine complexes,[6,7,11,12] in that the distance to the inner N atom (Pt−N2, 1.938(13) Å) is significantly shorter than those to the two outer N atoms (Pt−N1, 2.047(14) Å; Pt−N3, 2.013(13) Å). The trpy ligand is only slightly ruffled, the mean planes of the outer pyridine rings defining angles of 2.1 (N1 ring) and 3.2° (N3 ring) with that of the central pyridine ring. The Pt−N4 distance is 1.996(14) Å. This value is similar to the Pt−N (N of MeCN) distances of 1.977 and 1.981 Å for $Pt(MeCN)_2Cl_2$[10] and 1.94(2) Å for [Pt-(phbpy)(MeCN)]PF_6 (Hphbpy = 6-phenyl-2,2′-bipyridine).[13]

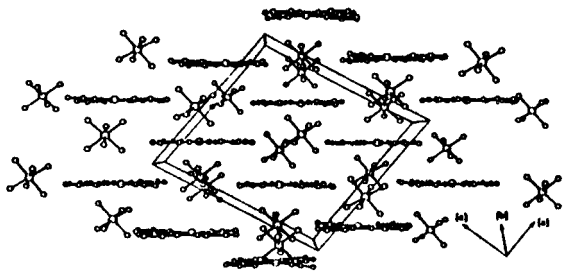

Figure 2. Packing diagram for $[Pt(trpy)(MeCN)](SbF_6)_2$.

Table 3. Selected Interatomic Distances (Å) and Angles (deg) for $[Pt(trpy)(MeCN)](SbF_6)_2$

	Distances		
Pt−N1	2.047(14)	Pt−N2	1.938(13)
Pt−N3	2.013(13)	Pt−N4	1.996(14)
N1−C1	1.32(2)	N1−C5	1.34(2)
N2−C6	1.35(2)	N2−C10	1.31(2)
N3−C11	1.36(2)	N3−C15	1.35(2)
N4−C16	1.08(2)	C1−C2	1.40(3)
C2−C3	1.32(3)	C3−C4	1.45(3)
C4−C5	1.39(3)	C5−C6	1.48(3)
C6−C7	1.39(3)	C7−C8	1.38(3)
C8−C9	1.33(3)	C9−C10	1.37(3)
C10−C11	1.47(2)	C11−C12	1.34(2)
C12−C13	1.37(3)	C13−C14	1.38(3)
C14−C15	1.36(3)	C16−C17	1.52(1)
	Angles		
N1−Pt−N2	81.8(6)	N1−Pt−N3	162.5(6)
N1−Pt−N4	98.3(6)	N2−Pt−N3	80.8(6)
N2−Pt−N4	179.3(5)	N3−Pt−N4	99.1(6)
Pt−N1−C1	128.6(13)	Pt−N1−C5	112.0(12)
Pt−N2−C6	116.6(12)	Pt−N2−C10	118.1(12)
Pt−N3−C11	113.0(11)	Pt−N3−C15	128.5(13)
Pt−N4−C16	179(2)	N4−C16−C17	177(2)

The crystal lattice consists of parallel sheets of cations and anions; Figure 2 gives a view of the packing parallel to these sheets. Within a sheet, the $[Pt(trpy)(MeCN)]^{2+}$ and SbF_6^- moieties reside in alternating rows of cations and anions which extend along the *b* axis. Since the planar cations lie side-by-side, there are no $\pi-\pi$ or metal−metal interactions along a row of cations. A *c*-glide plane relates successive sheets such that a row of anions lies directly above a row of cations. Thus, there are no extended interactions involving cations in a direction perpendicular to the sheets either. Specifically, the Pt−Pt distances between neighboring cations from adjacent sheets are all greater than 4.90 Å. Similarly, the intermolecular C(trpy)−C(trpy) distances are all greater than 3.5 Å and close to the upper limit of 3.8 Å for π aromatic interactions.[14] We conclude that the $[Pt(trpy)(MeCN)]^{2+}$ chromophore resides in a monomeric environment in the SbF_6^- salt and that this is a consequence of the cation:anion ratio of 1:2. Such a conclusion requires further verification, however, since this is the first

(11) Akiba, M.; Umakoshi, Y.; Sasaki, Y. *Chem. Lett.* **1995**, 607−608.

(12) Jennette, K. W.; Gill, J. T.; Sadowick, J. A.; Lippard, S. J. *J. Am. Chem. Soc.* **1976**, *98*, 6159−6168.

(13) Constable, E. C.; Henny, R. P. G.; Leese, T. A.; Tocher, D. A. *J. Chem. Soc., Chem. Commun.* **1990**, 513−515.

(14) Freyburg, D. P.; Robins, J. L.; Raymond, K. N.; Smart, J. C. *J. Am. Chem. Soc.* **1979**, *101*, 892−897.

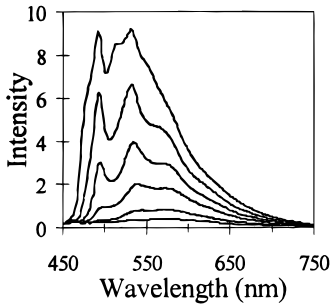

Figure 3. Solid-state emission spectra of [Pt(trpy)(MeCN)]$(SbF_6)_2$ recorded at 40 K intervals over the range 80−280 K. The emission intensity increases as the temperature decreases. The excitation wavelength was 350 nm.

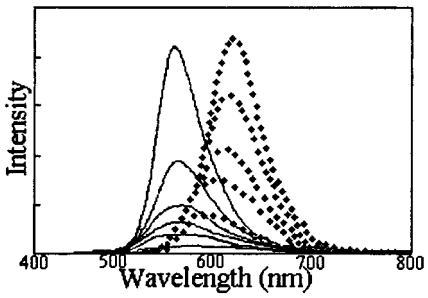

Figure 4. Emission spectra from solid-state samples of [Pt(trpy)Cl]-SbF_6 (left) and [Pt(trpy)Cl]CF_3SO_3 (right). In each case, the intensity increases as the temperature decreases. The temperatures are 100, 130, 160, 190, 220, and 280 K; there is no 220 K spectrum for the triflate compound. The excitation wavelength was 350 nm.

reported crystal structure determination of a terpyridyl salt of Pt(II) of 1:2 cation:anion stoichiometry.

Emission from [Pt(trpy)(MeCN)]$(SbF_6)_2$. In the solid state, the emission from [Pt(trpy)(MeCN)]$(SbF_6)_2$ clearly reflected different components at different temperatures (Figure 3). Thus, above ca. 240 K the principal emission maxima occurred at around 540 and 575 nm, respectively, and there were weaker emission maxima at ca. 495 and ca. 465 nm. From 200 K down to about 120 K, the overall intensity increased, but there was a change in the band shape. In this temperature regime, the band at 495 nm evolved into a dominant spectral feature along with the band at 530 nm, and both maxima shifted to somewhat shorter wavelengths. At the same time, the relative intensity of the band at 575 nm decreased, and it became a shoulder. Finally, at the lowest accessible temperature, ca. 80 K, the spectrum sharpened further and new shoulders appeared at about 480, 515, and 550 nm, respectively. At each temperature, the vibrational structure within the emission spectrum is consistent with a $^3\pi-\pi^*$ orbital parentage. Parenthetically, we may note that the apparent emission maximum at 465 nm in the room-temperature spectrum of Figure 3 could represent $^3\pi-\pi^*$ emission from coordinated trpy as well. However, it could also be an artifact, since the signal intensity changes very little at this wavelength over the entire temperature range investigated. A reviewer pointed out that reabsorption of the emission could be a factor influencing the observed band shape. However, experiments showed that, in the room-temperature, solid-state reflectance spectrum, the longest wavelength absorption band with any appreciable intensity had a maximum at about 390 nm and a tail that extended to only ca. 450 nm.

For comparison, we measured the emission from Pt(trpy)-$(MeCN)^{2+}$ in a butyronitrile glass at 77 K. The spectrum of the glass yielded well-resolved vibronic maxima, and the onset of the spectrum fell at a shorter wavelength. For a 150 μM solution, the emission maxima occurred at 457, 491, 529, and 565 nm.

Physical Data for the [Pt(trpy)Cl]A Solids. Like Bailey et al.,[7] we found that the emission spectrum of $[Pt(trpy)Cl]^+$ varied markedly with the counterion in the solid state as well as with the temperature. However, we often observed qualitatively different kinds of behavior. In our studies with SbF_6^- as the counterion, the compound was yellow and the maximum in the uncorrected emission spectrum occurred at 552 nm. Although the wavelength maximum of the emission was essentially independent of the temperature (Figure 4), the intensity increased as the temperature decreased. The room-temperature decay was not monoexponential, but the emission lifetime was about 750 ns in the tail of the decay curve. On the other hand, the decay was essentially monophasic at 77 K and had a lifetime of about 3 μs. Although Bailey et al. studied ostensibly the same chromophore as part of a yellow solid with PF_6^- as the counterion,[7] they found that the room-temperature emission maximum occurred at a much longer wavelength, ca. 630 nm. Moreover, at lower temperatures, emission occurred at shorter wavelengths and there was a decrease in the bandwidth. By around 100 K, the emission maximum stopped shifting and stabilized at about 565 nm.[7] Our preparation of the triflate salt gave an uncorrected emission maximum at 585 nm at 280 K. At lower temperatures, the emission maximum shifted to longer wavelengths, out to 613 nm at 100 K (Figure 4), in line with the results of Yip et al.[6]

Discussion

The [Pt(trpy)(MeCN)]$(SbF_6)_2$ System. The structured emission shown by the nitrile complex in the low-temperature glass or the solid state clearly represents ligand-centered $^3\pi-\pi^*$ emission. However, for the solid state, the emission appears at longer wavelengths and the spectrum is quite temperature dependent. At low temperature, new shorter-wavelength emission maxima appear in the solid-state spectrum, but even at 80 K, the emission does not attain the energy found from the glass. In principle, a phase transition could account for the temperature dependence of the emission spectrum; however, this is unlikely. One reason is that the data would require a series of phase changes at different temperatures. The other problem with this model is that the lowest energy emission occurs at room temperature, where the structure shows there are no significant neighbor−neighbor interactions, at least in the bulk material.

The most likely explanation of the data is that the emission originates from different trap sites depending on the temperature. The trap centers could be either defect sites or sites where the excitation itself generates a locally modified structure.[15] When energy transfer is facile in the solid, the chromophores in the bulk simply act as antennae that efficiently take up the energy which then flows into lower energy trap sites. Of course, the energy-distribution processes are temperature dependent and, at a sufficiently low temperature, the population of particular traps may no longer be feasible. Under these conditions, new, higher energy emission spectra appear at lower and lower temperatures. This model nicely accounts for the data, but the crucial assumption is that energy transfer occurs readily in the solid state. There are, however, good precedents for this behavior, particularly when the excitation involves IL excited states of aromatic ligands.[4,16−18] With IL excitation, the extent

(15) Blasse, G.; Grabmaier, B. C. *Luminescent Materials*; Springer-Verlag: New York, 1994; Chapter 3.
(16) Krol, D. M.; Blasse, G. *Chem. Phys. Lett.* **1981**, *77*, 253−256.
(17) Zillian, S.; Güdel, H. U. *Inorg. Chem.* **1992**, *31*, 830−835.
(18) Blanzat, B.; Barthou, C.; Tercier, N. *J. Am. Chem. Soc.* **1987**, *109*, 6193−6194.

of structural reorganization and the barrier to energy transfer are frequently minimal. Regarding the structure of the trap center, some type of intermolecular interaction such as trpy−trpy stacking is very likely to be responsible for the red shift in the solid-state emission spectrum. Miskowski and Houlding have proposed that interligand interactions of this type can give rise to very large red shifts as well as the loss of vibrational structure.[2] On the other hand, in their studies of platinum(II) isobiquinolines, Kato et al. reported finding much smaller red shifts and emission with residual vibrational structure.[19] Kato et al. also found that the ^{3}IL emission from a mixed-ligand, dicyanide derivative exhibited multiple origins, consistent with the possible participation of trap centers.

The [Pt(trpy)Cl]A Systems in the Solid State. Extended interactions often have a profound influence on the optical and electrical properties of platinum(II) complexes in the solid state.[1,20] In the [Pt(trpy)Cl]A systems, this is evident from the influence the anion A has on the color of the material, as the energy of the MMLCT absorption varies with the metal-metal separation.[1,20−23] In particular, the effective intermolecular separation is clearly larger in the case of the yellow SbF_6^- derivative compared with the orange $CF_3SO_3^-$ compound. Figure 4 shows that the same effect is evident in the emission spectra, where the emission appears at significantly longer wavelengths when triflate is the anion. Moreover, the shift increases at lower temperatures almost certainly because of a further decrease in the mean platinum−platinum separation.[23] In contrast, the emission from what is probably a monomeric platinum center in the SbF_6^- salt occurs at significantly higher energy, and the maximum is effectively temperature independent. In this context, it is worth noting that Bailey et al. found that the apparently very similar, yellow PF_6^- salt exhibited a much longer wavelength emission maximum at room temperature.[7] However, they also reported that the emission underwent a blue shift at lower temperatures, down to about 160 K, and that at still lower temperatures a new emission signal emerged with a maximum at ca. 565 nm. The important point is that their low-temperature emission signal paralleled the signal we observed from the SbF_6^- analogue. The simplist way to reconcile the data for the PF_6^- system is to assume that the longer-wavelength emission, which was no longer evident at 100 K, originated at a trap site. This phenomenon provides another explanation for the fact that similar platinum(II) materials, or even different preparations of the same material, may exhibit distinct emissions. As a further illustration, consider the [Pt(trpy)Cl]CF_3SO_3 system. We observed a red shift in the emission maximum at lower temperatures whereas Bailey et al. reported a blue shift for the same compound. However, both groups observed similar emission spectra at the lowest temperatures.

Acknowledgment. We acknowledge support of this work from the National Science Foundation through Grant CHE-9401238 (D.R.M.) and from the University of Natal and the South African Foundation for Research Development (J.S.F.). R.B. thanks the African Explosives and Chemical Industries for a postgraduate bursary. The authors also thank Clifford P. Kubiak for his efforts and support.

Supporting Information Available: Tables of complete atomic coordinates and isotropic thermal parameters, non-hydrogen anisotropic temperature factors, bond distances, and bond angles (7 pages). Ordering information is given on any current masthead page.

IC961068B

(19) Kato, M.; Sasano, K.; Kosuge, C.; Yamazaki, M.; Yano, S.; Kimura, M. *Inorg. Chem.* **1996**, *35*, 116−123.
(20) Thomas, T. W.; Underhill, A. E. *Chem. Soc. Rev.* **1972** *1*, 99−120.
(21) Wan, K. T.; Che, C. M.; Cho, K. C. *J. Chem. Soc., Dalton Trans.* **1991**, 1077−1080.
(22) Textor, M.; Oswald, H. R. *Z. Anorg. Allg. Chem.* **1974**, *407*, 244−256.
(23) Connick, W. B.; Henling, L. M.; Marsh, R. E.; Gray, H. B. *Inorg. Chem.* **1996**, *35*, 6261−6265.